

Synthesis of n-Butyl Lactate by Transition-Metal-Substituted Phosphotungstic Acid Salt

Ke Wu¹, Li Xu^{1,2}, Ling Xu¹, Lijuan Xie¹, Zongrui Liu^{1,*}

¹College of Chemistry and Chemical Engineering, Inner Mongolia University for Nationalities, Tongliao, China

²College of Chemistry, Northeast Normal University, Changchun, China

Email address:

liuzr716@163.com (Zongrui Liu)

*Corresponding author

To cite this article:

Ke Wu, Li Xu, Ling Xu, Lijuan Xie, Zongrui Liu. Synthesis of n-Butyl Lactate by Transition-Metal-Substituted Phosphotungstic Acid Salt. *Science Journal of Chemistry*. Vol. 6, No. 4, 2018, pp. 43-49. doi: 10.11648/j.sjc.20180604.12

Received: August 16, 2018; Accepted: September 13, 2018; Published: October 18, 2018

Abstract: Fatty acid ester perfume occupied an important position in food industry. The characteristics of them were variety, easy synthesis and low price. They were widely used in daily flavor, edible flavor and industrial flavor. POMs were a kind of strong acid bifunctional mild environment-friendly catalysts, their drawback was excellent solubility and could not be reused. Here, series of transition-metal-substituted phosphotungstate $K_6[PW_{11}O_{39}M^{II}(H_2O)]$ ($M = Cu, Co, Ni$) Lewis acid heterogeneous phase catalysts based on mono-lacunary-Keggin type $K_7[PW_{11}O_{39}]$ were prepared by stereoselective method, $K_6[PW_{11}O_{39}M^{II}(H_2O)]$ ($M = Cu, Co, Ni$) were abbreviated as $PW_{11}M^{II}(H_2O)$ ($M = Cu, Co, Ni$). They were characterized by FT-IR, PXRD and element analysis. The coordinating water of transition metal was Lewis acid catalytic sites after activated. When mole ratio of butanol and lactic acid was 2: 1, amount of $PW_{11}M^{II}(H_2O)$ ($M = Cu, Co, Ni$) was 0.125 g, volume of cyclohexane was 15 mL, the reaction temperature was 105°C, reaction time was 2 h, conversion rate of n-butyl lactate were in order: 85.9%, 79.6%, 66.3%. Activity of $PW_{11}X$ ($X = Cu, Co, Ni$) had no obvious changes after three times recycling. In addition, magnetic studies indicate that antiferromagnetic interactions exist in the three compounds.

Keywords: Transition-Metal-Substituted, Substituted Phosphotungstic Acid Salt, n-Butyl Lactate, Lewis Acid Catalysis

1. Introduction

Synthetic perfume especially ester synthetic perfume are the important materials for food industry, cosmetics and drugs manufacture industry. Strong inorganic acid such as H_2SO_4 is the classical acid catalyst for the industrial progress of synthesis of synthetic ester perfume. [1-3] As we all know, the shortage of process route are equipment corrosion serious, poor selectivity and complicated process. [4, 5] With the enhancement of awareness of environment protection, scientist are working on small corrosion performance, low price, high performance catalyst. [6-9]

Polyoxometalates (POMs), as a class of nanosized metal-oxo clusters composed of group VI (Mo and W) and group V (V, Nb and Ta) elements in their highest oxidation state, have received increasing attention owing to their aesthetically appealing structures and wide applications such as in the fields of magnetism, [10-12] catalysis, [13-20] and proton

conduction. [22-24] Due to their strong acidity and fast multielectron transformation activity, POMs can be employed as acid, redox and bifunctional (acid and redox) catalyst for organic reactions. As homogeneous catalyst, POMs possess high activity, good selectivity and mild operation conditions. But there are still some difficulties for solve the problem of separation and recycling of POMs catalyst.

Inspired by the properties of POMs, series heterogeneous catalyst $PW_{11}M^{II}(H_2O)$ ($M = Cu, Co, Ni$) were explored by introducing transition metal ($M = Cu, Co, Ni$) into mono-lacunary-Keggin type $K_7[PW_{11}O_{39}]$. When low-valent transition metal ions such as Cu^{2+} , Co^{2+} , Ni^{2+} replace tungsten atom form substituted saturated POMs, these low-valence metal ions usually coordinated with one or more coordination water molecules. After a simple heating and activation, the coordination water lost and M^{2+} become the Lewis acid catalytic center. The Lewis acid catalytic performance of $PW_{11}M^{II}(H_2O)$ ($M = Cu, Co, Ni$) has been investigated by their catalytic conversion rates for synthesis of n-butyl lactate.

2. Experiment

2.1. Materials and Methods

$K_7[PW_{11}O_{39}]$ was prepared according to the literature procedures. [25] Other chemicals were obtained commercially and used without further purification. Fourier transform infrared (FT-IR) spectra of skeletal vibration of materials were recorded using KBr flake on a SHIMADZU NICOLET AVATAR 370 DTGS spectrometer. Powder X-ray diffraction (PXRD) patterns were recorded on a Shimadzu XRD-6000 diffractometer system equipped with Ni-filtered Cu target $K\alpha$ -ray (operation at 40 kV, 40 mA, wavelength $\lambda = 0.15418$ nm). Diffractions were carried out in the ranges (2θ) of 5° to 80° at the scanning speed of $0.02^\circ / \text{min}$. The magnetic susceptibility data were obtained on a SQUID magnetometer (Quantum Design, MPMS-5) in the temperature range 2–300 K with applied field of 1000 Oe. GC analyses were performed on an Agilent 6820 instrument with a flame ionization detector. Elemental analyses for C, N, and H were performed on a Perkin-Elmer 2400 CHN elemental analyzer, and for Cu, Co, Ni, P, W were determined with a PLASMASPEC (I) ICP atomic emission spectrometer.

2.2. Preparation of $PW_{11}X$ ($X = \text{Cu, Co, Ni}$)

$K_6[PW_{11}O_{39}M^{\text{II}}(\text{H}_2\text{O})]$ ($M = \text{Cu, Co, Ni}$) were prepared according to the literature procedures. [26] Solution A: 6.0 g $K_7[PW_{11}O_{39}]$ solid samples were dissolved in 18.0 mL distilled water. Solution B: 0.41 g $\text{CuSO}_4 \cdot 5\text{H}_2\text{O}$ were dissolved in 5.0 mL distilled water, solution B was heated to $30\text{--}40^\circ\text{C}$ and slowly poured into solution A, the pH of mixed solution was adjusted to 5.0 with 1M HCl solution. Stirring for 30 min at $30\text{--}40^\circ\text{C}$, then mixed solution was cooled to room temperature and 6.0 g KCl was added. After stirring for 20 min, the shallow green precipitate $PW_{11}C^{\text{II}}(\text{H}_2\text{O})$ was filtered separation, washed with water and air-dried. Synthetic method of $PW_{11}Co^{\text{II}}(\text{H}_2\text{O})$ and $PW_{11}Ni^{\text{II}}(\text{H}_2\text{O})$ were similar to $PW_{11}Cu^{\text{II}}(\text{H}_2\text{O})$, excepted using $\text{CoSO}_4 \cdot 7\text{H}_2\text{O}$ and $\text{NiSO}_4 \cdot 6\text{H}_2\text{O}$ instead of $\text{CuSO}_4 \cdot 5\text{H}_2\text{O}$.

2.3. Catalytic Reaction

The esterification reaction was performed in a three-necked round-bottomed flask with appropriate mass of $PW_{11}^{\text{II}}(\text{H}_2\text{O})$ ($M = \text{Cu, Co, Ni}$). Then, reasonable volume ratio of butanol and lactic acid, and cyclohexane water-carrying agent were added with magnetic stirring, the device was equipped with thermometer refluxing condenser tube and water segregator in atmospheric pressure in several hours. The solution was heated to boil and refluxed until no water flowed off. The resultant solution was distilled and purified. Samples should be taken every half an hour, and the sample should be diluted with acetone, the yield of n-butyl lactate can be measured by GC analysis with sample diluted by acetone solution.

3. Results and Discussion

3.1. FT-IR Studies

The Fourier Transform infrared spectroscopy (FT-IR) of $PW_{11}M^{\text{II}}(\text{H}_2\text{O})$ ($M = \text{Cu, Co, Ni}$) between 4000 and 400 cm^{-1} with KBr pellet was showed in Figure 1. In which, the absorption in the region of $1060\text{--}510\text{ cm}^{-1}$ were attributed to characteristic vibration patterns of $[PW_{11}O_{39}]^{7-}$ unit. The absorption at 1060 cm^{-1} and 950 cm^{-1} were terminal $W = O_t$ (O_t was terminal O) vibrations. The absorption at 900 cm^{-1} was attributable to the center $W\text{--}O_b\text{--}W$ (O_c was center O atom) vibration. The absorption at 809 and 510 cm^{-1} were bridging $W\text{--}O_b\text{--}W$ (O_b was bridged O atom) vibration. The absorption at 1673 cm^{-1} was the vibrations of P P-O. The characteristic absorption at 3428 cm^{-1} derived from the O-H stretching vibration of H_2O .

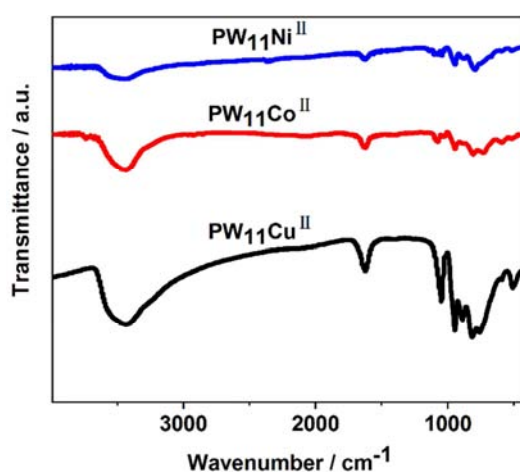


Figure 1. FT-IR patterns of catalysts.

3.2. XRD Studies

Figure 2 was PXRD patterns of $PW_{11}M^{\text{II}}(\text{H}_2\text{O})$ ($M = \text{Cu, Co, Ni}$) samples. All of those samples have perfectly confirmed with diffraction peaks of Keggin structure, whose 2θ were 28° , 48° and 58° , which indicated that $PW_{11}M^{\text{II}}(\text{H}_2\text{O})$ ($M = \text{Cu, Co, Ni}$) samples were isomorphic mono-substituted Keggin type POMs.

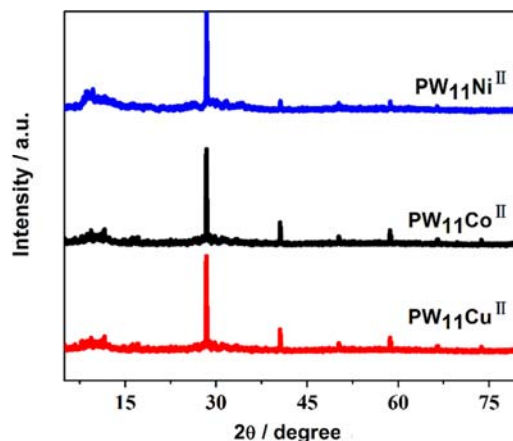


Figure 2. XRD patterns of catalysts.

3.3. Element Analysis

The $PW_{11}M^{II}(H_2O)$ ($M = Cu, Co, Ni$) solid samples were dissolved in 20 mL concentrated nitric acid (HNO_3) then was transferred to a Teflon-lined stainless-steel autoclave and sealed. After being heated at $120^\circ C$ for 24 h, it was cooled to room temperature and was transferred to 1L volumetric flask diluted into $1 \mu g/mL$ solution for elemental analysis. The experimental data were shown in Table 1.

Table 1. Elemental analysis for $PW_{11}M^{II}(H_2O)$ ($M = Cu, Co, Ni$).

Catalyst	Anal. Calcd / %	Found / %
$PW_{11}Cu$	H 0.07; O 21.38;	H 0.08; O 21.39;
	K 7.84; P 1.03;	K 7.82; P 1.02;
	W 67.56; Cu 2.12.	W 67.58; Cu 2.11.
$PW_{11}Co$	H 0.07; O 21.41;	H 0.07; O 21.43;
	K 7.85; P 1.04;	K 7.84; P 1.03;
	W 67.66; Co 1.97.	W 67.67; Co 1.96.
$PW_{11}Ni$	H 0.07; O 21.41;	H 0.06; O 21.40;
	K 7.84; P 1.04;	K 7.85; P 1.05;
	W 67.67; Ni 1.97.	W 67.65; Ni 1.99.

3.3. Chemical Stability Studies

In order to further detect chemical stability of $PW_{11}Cu^{II}(H_2O)$, $PW_{11}Co^{II}(H_2O)$ and $PW_{11}Ni^{II}(H_2O)$, PXRD of the three compounds were tested with different pH values (2-12) aqueous solution and different organic reagents. Soaking in the same volume of aqueous solution with pH range between 2-12 for 24 hours, as shown in Figure 3a, 3c, 3e, the PXRD peaks of the three compounds have no significant changes indicated that the three compounds were stable between the pH range of 2-12. Then soaking the three compounds in different organic solvent s (acetone, methanol, ethanol, dimdimethylformamide, n-butanol and lactic acid) with same volume after 24 hours then tested their PXRD. As shown in Figure 3b, 3d, 3f, PXRD peaks had no obvious changes compared with as-synthesized sample, which proved that the three compounds were stable in common organic solvents. All of experimental results shown that the three compounds were stable in these organic solvent (Figure 3b). The experimental results showed that the three compounds were chemical stable with strong acid and alkali aqueous solution and typical organic solvents.

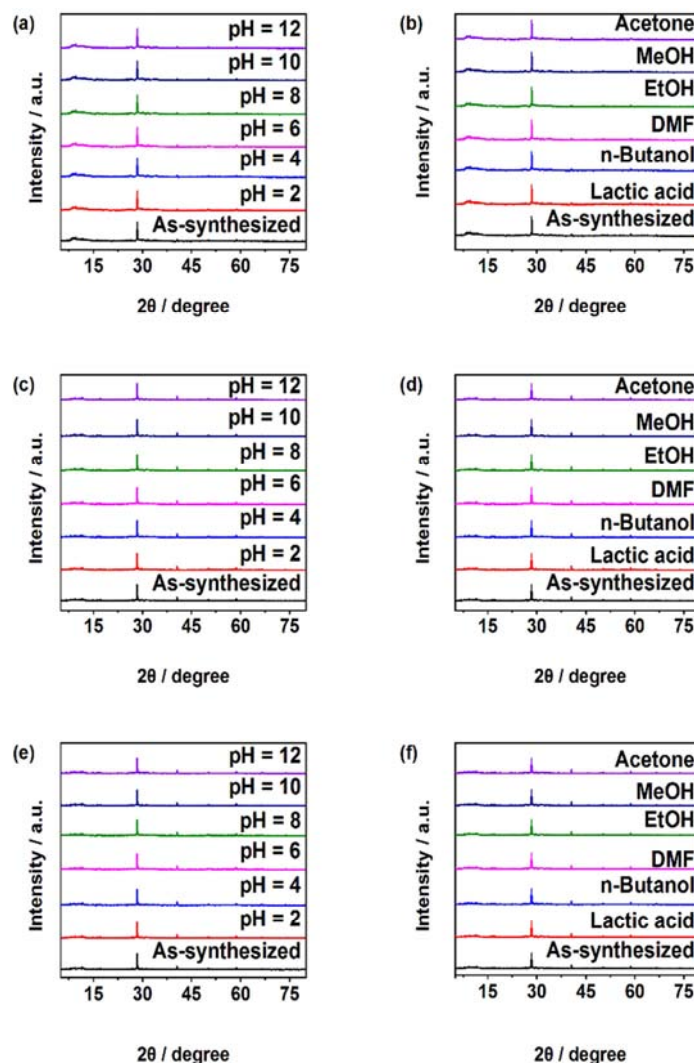


Figure 3. PXRD patterns of: (a) $PW_{11}Ni^{II}(H_2O)$ was disposed with pH values of aqueous solutions; (b) $PW_{11}Ni^{II}(H_2O)$ was soaked in different organic solvents; (c) $PW_{11}Co^{II}(H_2O)$ was disposed with pH values of aqueous solutions; (d) $PW_{11}Co^{II}(H_2O)$ was soaked in different organic solvents; (e) $PW_{11}Cu^{II}(H_2O)$ was disposed with pH values of aqueous solutions; (f) $PW_{11}Cu^{II}(H_2O)$ was soaked in different organic solvents.

3.4. Reaction Results

3.4.1. Effect on Esterification Rate at Different Ratio of Lactate Acid and Butyl Alcohol

When reaction time was 2 h, reaction temperature was 100°C, amount of $PW_{11}M^{II}(H_2O)$ ($M = Cu, Co, Ni$) was 0.125 g, amount of cyclohexane was 15 mL, molar ratio of butanol and lactic acid were 1.25:1, 1.5:1, 1.75:1, 2:1, 2.25:1, the effects of molar ratio of n-butanol and lactic acid on esterification rate showed in Figure 4. The conversion rate of $PW_{11}Cu^{II}(H_2O)$ were in order: 47.31%, 53.67%, 59.39%, 82.92%, 82.98%. The conversion rate of $PW_{11}Co^{II}(H_2O)$ were in order: 43.25%, 48.11%, 57.72%, 78.76%, 78.94%. The conversion rate of $PW_{11}Ni^{II}(H_2O)$ were in order: 39.76%, 43.75%, 53.19%, 64.39%, 63.97%. The activity of $PW_{11}M^{II}(H_2O)$ were $PW_{11}Cu^{II}(H_2O) > PW_{11}Co^{II}(H_2O) > PW_{11}Ni^{II}(H_2O)$. Conversion rate increases with increase of molar ratio of n-butyl alcohol and lactate acid. When conversion rate reached maximum, conversion rate did not increase with the increase of molar ratio of n-butyl alcohol and lactate acid, which might because effect of mole ratio of reaction equilibrium.

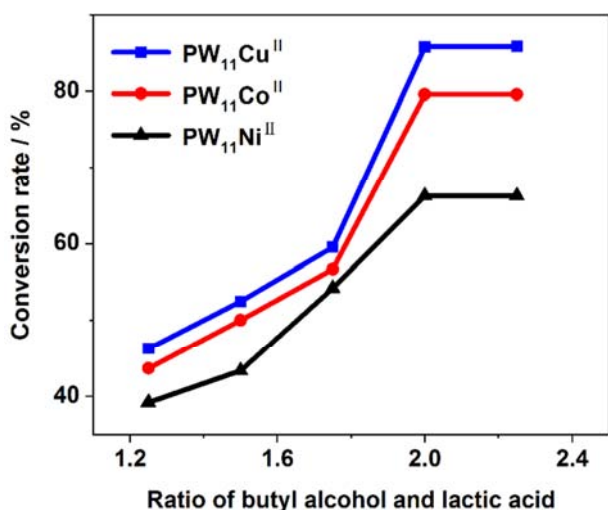


Figure 4. Effect on esterification rate at different ratio of butyl alcohol and lactate acid.

3.4.2. Effect of Amount of Catalyst on Esterification Rate

When reaction time was 2 h, reaction temperature was 100°C, molar ratio of butanol and lactic acid were 2:1, volume of cyclohexane was 15 mL, amount of $PW_{11}M^{II}(H_2O)$ ($M = Cu, Co, Ni$) was 0.125 g, effects of amount of $PW_{11}M^{II}(H_2O)$ ($M = Cu, Co, Ni$) on esterification rate shown in Figure 5. Conversion rate increases with increase of amount of $PW_{11}M^{II}(H_2O)$. When conversion rate reached maximum, conversion rate did not increase with increase of amount of catalysts, which might because the concentration of catalysts were too dense to reunite in the system lead to no further growth of conversion rate. The conversion rate of $PW_{11}Cu^{II}(H_2O)$ were in order: 58.96%, 45.73%, 81.97%, 84.98%, 83.67%. The conversion rate of $PW_{11}Co^{II}(H_2O)$ were in order: 49.16%, 63.71%, 73.86%, 77.29%, 79.91%. The conversion

rate of $PW_{11}Ni^{II}(H_2O)$ were in order: 36.36%, 53.19%, 57.96%, 66.17%, 66.03%. The activity of $PW_{11}M^{II}(H_2O)$ were $PW_{11}Cu^{II}(H_2O) > PW_{11}Co^{II}(H_2O) > PW_{11}Ni^{II}(H_2O)$.

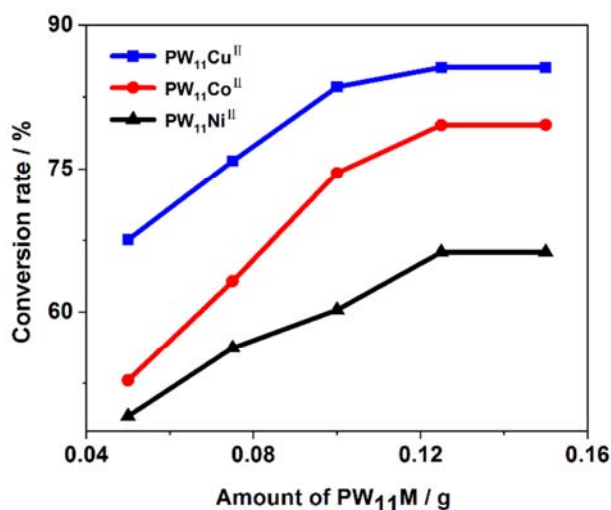


Figure 5. Effect of amount of catalyst on esterification rate.

3.4.3. Effect of Reaction Time on Esterification Rate

When reaction temperature was 100°C, molar ratio of butanol and lactic acid were 2:1, volume of cyclohexane was 15 mL, amount of $PW_{11}M^{II}(H_2O)$ ($M = Cu, Co, Ni$) was 0.125 g, reaction time was 1 h, 1.5 h, 2 h, 2.5 h, 3 h; Effects of reaction time on esterification rate showed in Figure 6. Conversion rate increases with increase of reaction time. When conversion rate reached maximum at 2.0 h, conversion rate did not increase with reaction time, which might because reaction equilibrium have been reached at 2 h. The conversion rate of $PW_{11}Cu^{II}(H_2O)$ were in order: 58.73%, 73.15%, 82.41%, 82.37%, 82.36%. The conversion rate of $PW_{11}Co^{II}(H_2O)$ were in order: 44.92%, 53.96%, 78.35%, 75.32%, 75.29%. The conversion rate of $PW_{11}Ni^{II}(H_2O)$ were in order: 31.93%, 46.79%, 63.99%, 64.01%, 63.97%. The activity of $PW_{11}M^{II}(H_2O)$ were $PW_{11}Cu^{II}(H_2O) > PW_{11}Co^{II}(H_2O) > PW_{11}Ni^{II}(H_2O)$.

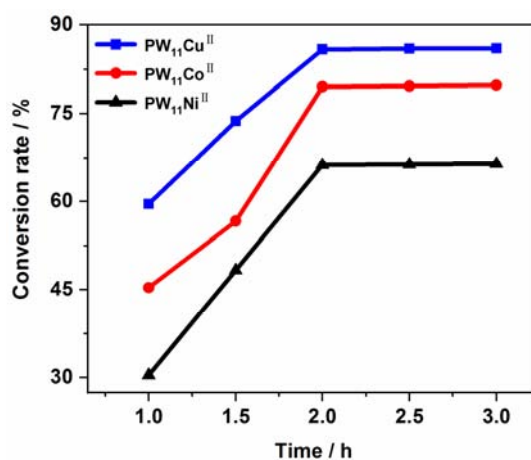


Figure 6. Effect of different reactional time on esterification rate.

3.4.4. Effect of Reaction Temperature on Esterification Rate

When reaction time was 2 h, molar ratio of butanol and lactic acid were 2:1, volume of cyclohexane was 15 mL, amount of $PW_{11}M^{II}(H_2O)$ ($M = Cu, Co, Ni$) was 0.125 g, reaction temperature was 90°C, 95°C, 100°C, 105°C, 110°C, the effects of reaction temperature on esterification rate showed in Figure 7. Conversion rate increases with increase of reaction time. When conversion rate reached maximum at 100°C, conversion rate did not increase with reaction temperature, which might because reaction equilibrium have been reached at 100°C. The conversion rate of $PW_{11}Cu^{II}(H_2O)$ were in order: 47.92%, 61.38%, 82.59%, 82.53%, 82.52%. The conversion rate of $PW_{11}Co^{II}(H_2O)$ were in order: 44.16%, 58.46%, 78.17%, 78.13%, 78.11%. The conversion rate of $PW_{11}Ni^{II}(H_2O)$ were in order: 36.03%, 51.07%, 66.18%, 66.16%, 66.13%. The activity of $PW_{11}M^{II}(H_2O)$ were $PW_{11}Cu^{II}(H_2O) > PW_{11}Co^{II}(H_2O) > PW_{11}Ni^{II}(H_2O)$.

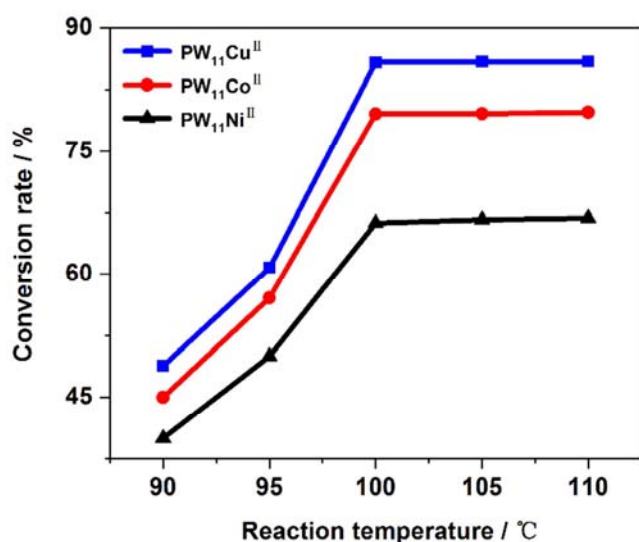


Figure 7. Effect of different temperature on esterification rate.

3.4.5. Effect of Volume of Cyclohexane on Esterification Rate

When reaction time was 2 h, molar ratio of butanol and lactic acid were 2:1, amount of $PW_{11}M^{II}(H_2O)$ ($M = Cu, Co, Ni$) was 0.125 g, reaction temperature was 100°C, volume of cyclohexane was 9 mL, 12 mL, 15 mL, 18 mL, 24 mL, effect of volume of cyclohexane on esterification rate showed in Figure 8. Conversion rate increases with increase of reaction time. When conversion rate reached maximum with 15 mL cyclohexane, conversion rate decrease with the increase of volume of cyclohexane, which might because too much cyclohexane might lead to decrease of concentration of catalyst. The conversion rate of $PW_{11}Cu^{II}(H_2O)$ were in order: 52.65%, 67.46%, 82.98%, 59.61%, 56.37%. The conversion rate of $PW_{11}Co^{II}(H_2O)$ were in order: 45.13%, 61.39%, 77.95%, 57.93%, 48.97%. The conversion rate of $PW_{11}Ni^{II}(H_2O)$ were in order: 43.43%, 57.39%, 62.09%, 51.93%, 32.87%. The activity of $PW_{11}M^{II}(H_2O)$ were $PW_{11}Cu^{II}(H_2O) > PW_{11}Co^{II}(H_2O) > PW_{11}Ni^{II}(H_2O)$.

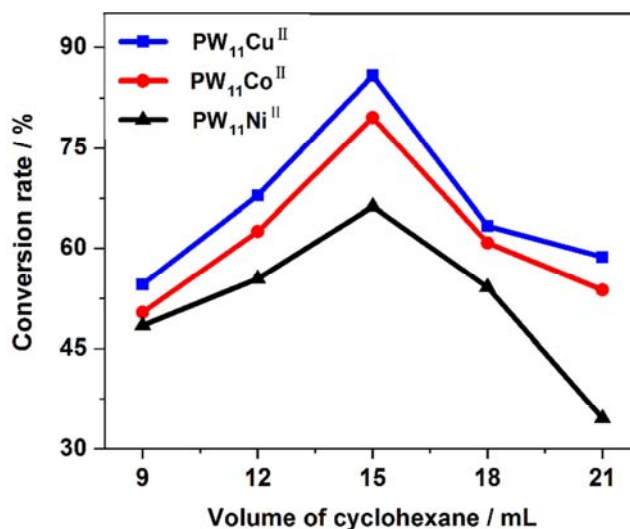


Figure 8. Effect of different volume of cyclohexane on esterification rate.

3.4.6 Recycling of Catalysts

The results of recycling test of $PW_{11}M^{II}(H_2O)$ ($M = Cu, Co, Ni$) were listed in Table 2. Activity of $PW_{11}M$ ($M = Cu, Co, Ni$) had no obvious changes after three times recycling exhibited that they were stable Lewis acid catalyst.

Table 2. Recycling experiment.

Catalyst	Times		
	1	2	3
$PW_{11}Cu$	83.4	82.4	81.9
$PW_{11}Co$	79.9	79.3	78.4
$PW_{11}Ni$	65.3	64.2	64.0

3.4.7. Hot Filtration Experiment

At the best reaction conditions: reaction time was 2 h, reaction temperature was 100°C, amount of $PW_{11}M^{II}(H_2O)$ ($M = Cu, Co, Ni$) was 0.125 g, amount of cyclohexane was 15 mL, molar ratio of butanol and lactic acid were 2:1 with hot filtration experiment. After 30 min of reaction, the catalysts were removed through hot filtration and the filtrate was further heated for 2 h at 100°C. As shown in Figure 9, there were no further growth of the conversion indicated that they were heterogeneous catalysts in the catalytic reaction and were not dissolved in the reaction system.

3.5. Magnetic Property

The temperature dependence of magnetic susceptibility of $PW_{11}M^{II}(H_2O)$ ($M = Cu, Co, Ni$) was investigated at 2–300 K in an applied magnetic field of 1000 Oe. Because the molecular structures of the three compounds were very similar, take $PW_{11}Cu^{II}(H_2O)$ as an example to introduce their properties. As shown in Figure 10(a), the M versus T plot demonstrated the M value slowly increases from 0.0071 emu mol⁻¹ at 300 K to 0.087 emu mol⁻¹ at 26 K, and then exponentially reached the maximum value of 0.63 emu mol⁻¹ at 2 K. The M/T value of 1 is 2.82 emu K mol⁻¹ at 300 K (Fig. 4), which is larger than the theoretical value of 1.125 emu K mol⁻¹ expected from three isolated

Cu^{2+} ($S = 0.5$, $g = 2.0$). As the temperature is lowered, the $\chi_M T$ value decreases slowly up to 0.186 at 50 K and then sharply falls to a minimum value of 0.0063 emu K mol^{-1} at 2 K. The temperature dependences of χ_M and $\chi_M T$ versus T plots for 1 suggest the presence of antiferromagnetic coupling interactions between Cu^{2+} centers. As shown in

Figure 10(b), the χ_M^{-1} versus T plot follows the Curie-Weiss law with $C = 2.98 \text{ emu K mol}^{-1}$ and $\theta = -22.37 \text{ K}$ in the range of 48–300 K, which further demonstrated the presence of antiferromagnetic interactions between Cu^{2+} ions in $\text{PW}_{11}\text{Cu}^{\text{II}}(\text{H}_2\text{O})$.

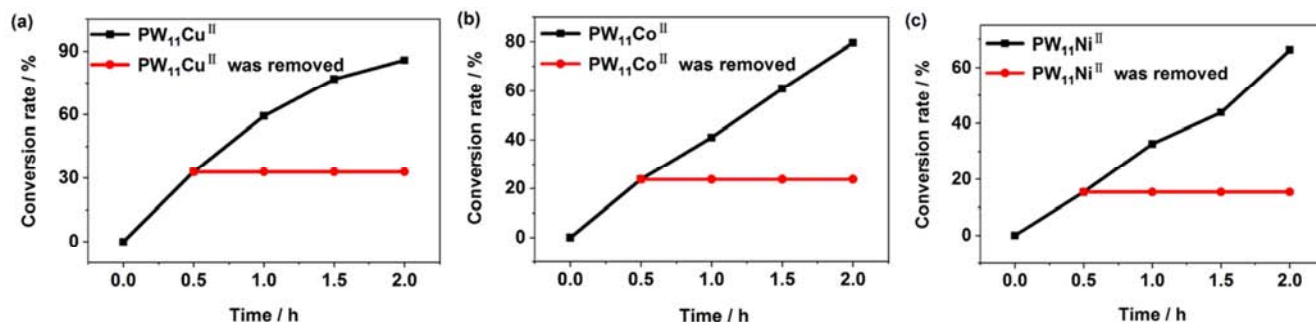


Figure 9. (a) (b) (c) Conversion rate versus time curves with $\text{PW}_{11}\text{M}^{\text{II}}(\text{H}_2\text{O})$ ($M = \text{Cu}, \text{Co}, \text{Ni}$) as catalyst at 100°C and catalyst was removed from the suspension after 30 min.

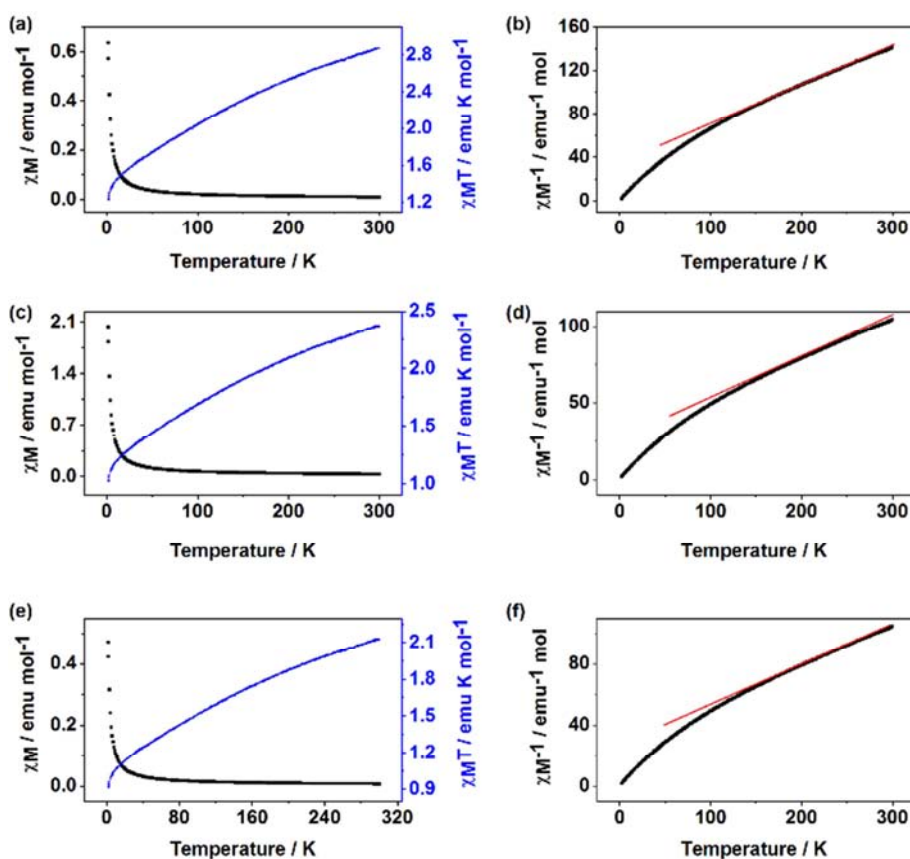


Figure 10. (a) (c) (e) The plots of χ_M and $\chi_M T$ vs T in temperature of 2–300 K for $\text{PW}_{11}\text{M}^{\text{II}}(\text{H}_2\text{O})$ ($M = \text{Cu}, \text{Co}, \text{Ni}$); (b)(d)(f) The plots of χ_M^{-1} vs T in temperature of 2–300 K for $\text{PW}_{11}\text{M}^{\text{II}}(\text{H}_2\text{O})$ ($M = \text{Cu}, \text{Co}, \text{Ni}$).

4. Conclusion

In summary, series of transition-metal-substituted phosphotungstate K_6 [$\text{PW}_{11}\text{O}_{39}\text{M}^{\text{II}}(\text{H}_2\text{O})$] ($M = \text{Cu}, \text{Co}, \text{Ni}$) based on mono-lacunary-Keggin type K_7 [$\text{PW}_{11}\text{O}_{39}$] were synthesized by stereoselective method. They were chemically stable with strong acid aqueous solution and typical organic solvents. These compounds owned Lewis acid active sites

after heating activation. They showed good Lewis acid activities for synthesis of n-butyl lactate, in which, The Lewis acid activity of them were $\text{PW}_{11}\text{Cu}^{\text{II}}(\text{H}_2\text{O}) > \text{PW}_{11}\text{Co}^{\text{II}}(\text{H}_2\text{O}) > \text{PW}_{11}\text{Ni}^{\text{II}}(\text{H}_2\text{O})$. The catalytic performance was stable after recycling three times. The presence of antiferromagnetic interactions between Cu^{2+} , Co^{2+} and Ni^{2+} ions in $\text{PW}_{11}\text{M}^{\text{II}}(\text{H}_2\text{O})$ ($M = \text{Cu}, \text{Co}, \text{Ni}$).

Acknowledgements

The authors acknowledged the financial support of the National Natural Science Foundation of China (No. 21661026).

References

- [1] L. H. Zhang, Y. W. Tian. "Synthesis of trimethylolpropane tris-acrylate catalyzed by calcium sulfate whisker. *J Mol. Sci.*, 2009, 25, (6): 375-378.
- [2] X. W. Kong, Z. J. Li, F. Yan, et al. Synthesis of ethylene glycol monopelargonate with Silica supported sodium bisulfate as catalyst. *J Mol. Sci.*, 2010, 26 (3): 208-212.
- [3] D. Y. Chen, J. P. Wang, Y. Bo. Survey of synthesis of lactic esters and its derivatives. *Chem. Ind. Eng. Prog.*, 2002, 21 (4): 243-246.
- [4] A. S. H. Kumar, K. T. V. Rao, K. Uppendar, et al., Nitration of Methyl 5-Nitrosalicylate Catalyzed by $H_6PMoV_3O_{40}$ Supported on Silica Gel. *Catal. Comm.*, 2012, 18: 37-40.
- [5] S. Mallick, K. M. Parida, Selective Nitration of Phenol over Silicotungstic Acid Supported Zirconia. *Catal. Comm.*, 2007, 8(10): 1487-1492.
- [6] S. J. Feng, L. Zhang, Y. H. Ren, et al., Catalytic Hydroxylation of Benzene to Phenol with Hydrogen Peroxide over Cesium Salts of Keggin-type Heteropoly Acids. *Acta Chim Sin*, 2012, 70(22): 2316-2322.
- [7] E. Rafiee, M. Joshaghani, F. Tork, et al., Esterification of Mandelic Acid Catalyzed by Heteropoly Acid. *J Mol Catal A: Chem*, 2008, 283(1/2): 1-4.
- [8] A. Shaabani, M. Behnam, A. H. Rezayan, Tungstophosphoric Acid ($H_3PW_{12}O_{40}$) Catalyzed Oxidation of Organic Compounds with $NaBrO_3$. *Catal. Comm*, 2009, 10(7): 1074-1078.
- [9] M. N. Timofeeva, Acid Catalysis by Heteropoly Acids. *Appl. Catal. A*, 2003, 256(1/2): 19-35.
- [10] X. B. Han, Z. M. Zhang and Zhang T. "Polyoxometalate-based cobalt-phosphate molecular catalysts for visible light-driven water oxidation," *J. Am. Chem. Soc.*, 2014, 136 (14): 5359-5366.
- [11] Z. Zhang, Q. Lin, and D. Kurunthu. "Synthesis and photocatalytic properties of a new heteropolyoxoniobate compound: $K_{10} [Nb_2O_2(H_2O)_2] [SiNb_{12}O_{40}] \cdot 12H_2O$," *J. Am. Chem. Soc.*, 2011, 133(18): 6934-6937.
- [12] B. Schwarz, J. Forster and M. K. Goetz. "Visible-light-driven water oxidation by a molecular manganese vanadium oxide cluster," *Angew. Chem. Int. Ed.*, 2016, 55 (21): 6329-6333.
- [13] X. B. Han, Li Y G, and Z. M. Zhang. "Polyoxometalate-based nickel clusters as visible light-driven water oxidation catalysts," *J. Am. Chem. Soc.*, 2015, 137 (16): 5486-5493.
- [14] M. Raula, G. G. Or and M. Saganovichl. "Polyoxometalate complexes of anatase-titanium dioxide cores in water," *Angew. Chem. Int. Ed.*, 2015, 54 (42): 12416-12421.
- [15] L. Yu, X. Du and Y. Ding. "Efficient visible light-driven water oxidation catalyzed by an all-inorganic copper-containing polyoxometalate," *Chem. Comm.*, 2015, 51 (98): 17443-17446.
- [16] K. Suzuki, M. Sugawa and Y. Kikukawa. "Strategic Design and Refinement of Lewis Acid-Base Catalysis by Rare-Earth-Metal-Containing Polyoxometalates," *Inorg. Chem.*, 2012, 51(12): 6953-6961.
- [17] K. Kamata, T. Yamaura and Mizuno N. "Chemo- and Regioselective Direct Hydroxylation of Arenes with Hydrogen Peroxide Catalyzed by a Divanadium-Substituted Phosphotungstate," *Angew. Chem. Int. Ed.*, 2012, 51(29): 7275-7278.
- [18] Ishimoto R., Kamata K. and N. Mizuno. "A Highly Active Protonated Tetranuclear Peroxotungstate for Oxidation with Hydrogen Peroxide," *Angew. Chem. Int. Ed.*, 2012, 51(19): 4662-4665.
- [19] Y. Kikukawa, Y. Kuroda and K. Yamaguchi. "Diamond-Shaped $[Ag_4]^{4+}$ Cluster Encapsulated by Silicotungstate Ligands: Synthesis and Catalysis of Hydrolytic Oxidation of Silanes," *Angew. Chem. Int. Ed.*, 2011, 51(10): 2434-2437.
- [20] L. Xu, Y. Lu and L. P. Huang. "Synthesis and Properties of a POMs-based Trinuclear Copper(II) Triazole Framework," *RSC Adv*. 2018, 8(4), 2034-2041.
- [21] J. Li, X. L. Cao and Y. Y. Wang. "The Enhancement on Proton Conductivity of Stable Polyoxometalate-Based Coordination Polymers by the Synergistic Effect of MultiProton Units," *Chem-A Eur. J.*, 2016, 22(27): 9299-9304.
- [22] X. Y. Lai, Y. W. Liu and G. C. Yang. "Controllable proton-conducting pathways via situating polyoxometalates in targeting pores of a metal-organic framework," *J. Mat. Chem. A*, 2017, 5(20): 9611-9617.
- [23] E. L. Zhou, C. Qin and X. L. Wang. "Steam-Assisted Synthesis of an Extra-Stable Polyoxometalate-Encapsulating Metal Azolate Framework: Applications in Reagent Purification and Proton Conduction," *Chem-A Eur. J.*, 2015, 21(37): 13058-13064.
- [24] M. L. Wei, X. Wang and X. Duan. "Crystal Structures and Proton Conductivities of a MOF and Two POM-MOF Composites Based on Cu(II) Ions and 2,2'-Bipyridyl-3,3'-dicarboxylic Acid," *Chem-A Eur. J.*, 2013, 19(5): 1607-1616.
- [25] N. Haraguchi, Y. Okaue and T. Isobe. "Stabilization of Tetravalent Cerium upon Coordination of Unsaturated Heteropoly tungstate Anions," *Inorg. Chem.*, 1994, 33(6): 1015-1020.
- [26] Q. J. Shan. Synthesis of n-butyl acetate by transition metal mono-substituted tungstophosphoric heteropoly acid catalyst [J]. *Chemical industry times*, 2013, 27(7). 31-33.